行政院國家科學委員會專題研究計畫　成果報告

奈米相變之鈦酸鍶鋇薄膜在微熱感測元件之應用

計畫類別：個別型計畫
計畫編號：NSC91-2218-E-009-007-
執行期間：91 年 08 月 01 日至 92 年 10 月 31 日
執行單位：國立交通大學電子工程學系

計畫主持人：鄭晃忠

計畫參與人員：郭孟維,詹爵魁,王志良,史德智(國立交通大學電子工程學系)

報告類型：精簡報告
報告附件：出席國際會議研究心得報告及發表論文
處理方式：本計畫可公開查詢

中　華　民　國 92 年 10 月 31 日

行政院國家科學委員會補助專題研究計畫成果報告

※※※※※※※※※※※※※※※※※※※※※※※※※
※ ※
※ 奈米相變之鈦酸鍶鋇薄膜在微感測元件之應用 ※
※ ※
※ ※
※※※※※※※※※※※※※※※※※※※※※※※※※

計畫類別：■個別型計畫 □整合型計畫
計畫編號：NSC 91-2218-E-009-007
執行期間： 91 年 8 月 1 日至 92 年 10 月 31 日

計畫主持人：鄭晃忠 國立交通大學電子工程學系
共同主持人：

計畫參與人員：郭孟維、詹爵魁、王志良、史德智
國立交通大學電子工程學系

本成果報告包括以下應繳交之附件：
□赴國外出差或研習心得報告一份
□赴大陸地區出差或研習心得報告一份
■出席國際學術會議心得報告及發表之論文各一份
□國際合作研究計畫國外研究報告書一份

執行單位：國立交通大學電子工程學系

中 華 民 國 92 年 10 月 31 日

奈米相變之鈦酸鍶鋇薄膜在微感測元件之應用

Application of thin (Ba,Sr) TiO_3 films with nano-phase transition for micro-thermistor

計畫編號：NSC 91-2218-E-009-007
執行期限：91 年 8 月 1 日至 92 年 10 月 31 日
主持人：鄭晃忠　國立交通大學電子工程學系
計畫參與人員：郭孟維、詹爵魁、王志良、史德智
國立交通大學電子工程學系

中文摘要

鈦酸鍶鋇由於具有高介電常數以及壓電性，熱電性等特點，近來廣泛應用在動態隨機存取記憶體的電容器以及各種感測元件上面。在溫度感測器方面則是利用相變時，介電常數或電阻發生巨大變化，偵測電容或電流變化以得知溫度的變化。首先，我們將鈦酸鍶鋇薄膜濺鍍在 Pt/TiN/Ti/Ox 的基板上面，接著濺鍍 Pt 為上電極，形成金屬/絕緣層/金屬(MFM)的結構，再經過不同溫度的快速熱退火處理之後，進行電性量測。我們改變量測時的基板溫度，以得知溫度對於鈦酸鍶鋇薄膜電性上的影響。我們發現鈦酸鍶鋇薄膜具有不錯的正溫度電阻效應，(並可以 Heywang model 來加以解釋)，這在熱敏電阻及微感測元件的運用上，是很有利的

Abstract

Ferroelectric materials with high dielectric constant, pyroelectricity and piezoelectricity have recently been extensively applied on DRAM capacitors and sensors. For applications on sensors, large variations of dielectric constant and resistivity of BST thin films with temperature during phase transition are used to improve sensitivity. The BST thin films with low crystallization temperature were deposited onto the Pt/TiN/Ti/Ox/Si substrate by rf magnetron sputter at 300°C substrate temperature. The BST thin films were then post annealed by rapid thermal annealing (RTA). Finally, physical and electrical properties of the BST thin films were investigated. In our experiments, BST thin films revealed positive TCR (PTCR) effect, which can be applied on thermal sensors.

Reasons and Purposes

During the past decades, high temperature coefficient resistivity (TCR) materials have been widely investigated and applied on thermistors as thermal detectors or infrared sensors due to their low cost and excellent thermal response. [1] There are two kinds of these TCR materials: positive temperature coefficient resistivity (PTCR) and negative temperature coefficient resistivity (NTCR). Of these materials, $BaTiO_3$ (BTO) is the most famous. The abnormally high positive TCR of BTO ferroelectric materials, observed at the Curie temperature (T_c) in 1955 [2], have attracted much attention to their applications and conduction mechanisms. Thermal detectors that use PTCR material can prevent the effect of thermal runaway, so the complementary

circuits can be greatly simplified [3]. The substitution of Sr for Ba in BTO solid solution, forming $(Ba,Sr)TiO_3$, can adjust the Curie Temperature to obtain proper operation condition of a thermistor, ex: at room temperature. Techniques for fabrication microelectro-mechanical systems (MEMs) and integrated circuits (ICs) are generally applied to high TCR microthermistors [4]. However, a low thermal budget process must be implemented to prevent damage to the underlayer structures of MEMs and the embedded ICs. In this work, the BST films were post-annealed by rapid thermal annealing system (RTA), which is a low-thermal-budget technique, to yield excellent electrical properties. Many studies have considered the TCR effect of bulk BST, but few have reported the TCR effect of thin BST films [1][5]. The conduction current of a BST was measured at temperature ranging from room temperature to 410 K, and the conduction mechanisms were investigated systematically.

Experiments

$Ba_{0.8}Sr_{0.2}TiO_3$ film (300nm) was deposited on Pt/TiN/Ti using a radio-frequency (rf) magnetron co-sputtering system at a substrate temperature of 300^{o}C. The rf powers used to deposit $BaTiO_3$ and $SrTiO_3$ were 185 W and 185 W, respectively, yielding a Ba/Sr ratio of 8:2. The BST films were subsequently post-treated by RTA system at O_2 ambient with different temperature and different time. Finally, the Pt top electrode of 100nm was deposited onto the BST film. The crystallinity was then characterized by X-ray diffraction (XRD, Siemens D5000 diffractometer). The XRD patterns show the polycrystalline nature of the perovskite BST formed in this work. The current-temperature characteristic was studied using the Pt/BST/Pt (metal-insulator-metal, MIM) structure, as shown in Fig. 1. Then, the testing voltage was biased on the top electrode, and the bottom electrode was grounded. An automatic measurement system, combining an HP4156C and a probe station, was employed to obtain the current- voltage (I-V) characteristic of the BST resistors. The current-temperature testing was carried out using a hot plate.

Results and Discussion

The TCR is defined according to the following formulas [4][6]:

$$TCR = \frac{1}{R_s}\frac{dR_s}{dT}\bigg|_T \qquad (1)$$

where T and R_s represent the temperature and the resistance, respectively. Fig. 2 plots the resistances and TCR characteristics of BST films without post-treatment, and with post RTA treatments at 400, 500 or 600^{o}C at –3V. The resistances of all these films polarized at a negative bias decreases as temperature increase. Hence, these negative polarized films behave negative TCR (NTCR), which is greatly enhanced for the BST films post-treated by RTA at 400, 500 and 600^{o}C. A maximum NTCR as high as 13.8% was achieved at a bias of –3 V for the RTA 400^{o}C sample. However, the RTA 500 and 600^{o}C samples show different TCR trends due to

the differences in R_s, as calculated in Eq. 1. Generally, the conduction current of BST film is induced by the presence of oxygen vacancies according to the equation:

$$O_o \leftrightarrow V_o^{2+} + 2e^- + \frac{1}{2}O_2 \qquad (2)$$

where O_o, V_o^{2+}, and e^- denote the oxygen ion on its normal site, an oxygen vacancy, and electron, respectively. High concentration of oxygen vacancies led to n-type conductivity of the BST materials due to the electrons generated, causing large conduction currents. However, at lower RTA temperature, the damage induced by thermal stress due to rapid temperature change is slight. Besides, the O_2 ambient during RTA compensates oxygen vacancies effectively. Thus the conductivity is suppressed. On the other hand, when the RTA temperature increases, the thermal stress and oxygen vacancies, which will degrade the BST films, are more severe. The crystallinity of the BST films is also improved obviously at higher RTA temperature. Therefore, the conductance of BST films increases with RTA temperature at higher RTA temperature.

The conduction mechanisms of metal/ferroelectric/metal (MFM) resistors are usually interpreted as interface-limited and bulk-limited conductions.[7][8] Generally Schottky emission (SE) governs the interface-limited current in the Pt/BST films, and the leakage current is expressed as

$$J_{SE}=A^*T^2\exp\{-q[\phi_B-(qE/4\pi\varepsilon_d\varepsilon_0)^{1/2}]/kT\} \qquad (3)$$

(where A^* is the effective Richardson's constant, φ_B is the potential barrier height at the surface, ε_d is the dynamic dielectric constant of the ferroelectric material in the infrared region, q is the unit charge, k is Boltzmann's constant, T is temperature, and E is the external electric field). If the conduction current is governed by SE behavior, then $\log(J/T^2)$ against $E^{1/2}$ and 1/t plots should be linear. Fig. 3 illustrates the $\mathrm{Log}(J/T^2)$ vs. $E^{1/2}$ curves of BST films without post treatment and post treated at 400, 500, and 600°C, respectively. Clearly, $\mathrm{Log}(J/T^2)$ increases linearly with the increase of $E^{1/2}$, thus we can attribute the conduction mechanism of BST films under negative bias as Schottky emission. Fig. 4 presents the resistances and the TCR characteristics of the BST films polarized at a positive bias. The BST films without RTA treatment and with RTA treatment at 400°C exhibit NTCR at +3 V, as shown in Fig. 4(a) and (b), but for the films treated with RTA 500 and 600°C reveal positive TCR (PTCR) in a temperature range for measuring temperature from 300 to 373K, as shown in Fig. 4(c) and (d). In Fig. 5 and Fig. 6, we have presented that BST films post treated with RTA at 500 and 600°C do not exhibit SE behavior under positive bias at all.

The electron energy bands explain the NTCR/PTCR effects of the RTA-treated BST films under negative/positive bias, as presented in Fig. 7 and Fig. 8. The BST films post-annealed by RTA in oxygen ambient are greatly improved due to compensation for oxygen vacancies at the upper surface; accordingly, SE behavior dominates the conduction current at a negative bias, as indicated in Fig. 7. Hence, the negative-biased conduction current exhibits an NTCR effect according to the

current-temperature relation of Eq. 3. However, the BST/Pt films treated by RTA at high temperature (>500^{o}C) are subject to a large thermal stress due to the abrupt fall in temperature, and thus many defects are induced at the interface of BST/Pt-bottom-electrode interface. The thermal-stress-induced interface states generated the injected electron current. Thus, the conduction current of BST film post-treated by RTA treatment is bulk limited under positive bias, as indicated in Fig. 8. Generally, the barrier scattering or the charge-detrapping rate governs bulk-limited current. [9][10] The current-temperature relationship for the grain boundary scattering is deduced using the Heywang formula at around the transition temperature (T_c) for ferroelectric materials according to [1][10]

$$R_s \propto \exp(-q\phi / kT) \quad , \quad \phi = \frac{e^2 N_d d^2}{2\varepsilon\varepsilon_0} \qquad \textbf{(4)}$$

where R_s is the resistance of the sample; ϕ and d are the potential height and depletion width at grain boundaries; ε and N_d present the electron mobility and the donor concentration in the films, and k is the Boltzmann constant. The barrier height according to the Heywang model increases with temperature. The Heywang barrier scattered the injected-current at a positive bias, and thus this bulk-limited current exhibits the PTCR phenomenon.

Conclusions

In this work, all the Pt/BST/Pt thin films polarized at negative bias reveal NTCR behavior, but the RTA-treated samples polarized at positive bias exhibit PTCR behavior. The leakage current of the samples with RTA treatment increased due to increasing oxygen vacancies, but all the samples formed Schottky barrier because the O_2 ambient gas compensated oxygen vacancies at upper surfaces. Hence, SE dominates the conduction current of tha samples biased at negative voltage, inducing the NTCR phenomenon. RTA treatment results in a steep gradient of the temperature decrease across the interface between the bottom electrode and the BST film, and thus induces residual thermal stress. The injected electron current is therefore formed by the thermal-stress-induced interface states at positive bias, and this bulk-limited current is governed by Heywang barrier scattering. Hence, the positive biased RTA-treated BST film exhibits the PTCR phenomenon.

Reference

1. K. Uchino, “Ferroelectric Devices”, pp. 243, Marcel Dekker, Inc., New York, 2000
2. O. Saburi, “Properties of semiconductive barium titanates”, *J. Phys. Soc. Jpn.*, vol. **14**, pp. 1159-1174, 1959.
3. L. Wang, “A New Smart Material-Multilayer PTC Thermistor”, *IEEE Trans. Compon., Packag. Manuf. Technol., Part A*, vol. **18**, pp. 249, 1995.
4. J. S. Shie, “Characterization and modeling of metal-film microbolometer”, *J. Microelectromech. Syst.*, vol. **5**, pp. 298-306, 1996.
5. H. Ihrig, “PTC effect in $BaTiO_3$ as a function of doping with 3d elements”, *J. American Ceramic Society.*, vol. **64**, No. 10, pp. 617-620, 1981.
6. T. Mori, “Vacuum-encapsulated thermistor bolometer type miniature infrared sensor”, *J. Microelectromech. Syst.*, vol. **3**, pp. 257-262, 1994.
7. C. S. Hwang, et. al., “A comparative study on the electrical conduction mechanisms of $(Ba_{0.5}Sr_{0.5})TiO_3$ thin films on Pt and IrO_2 electrodes”, *J. Appl. Phys.*, vol **83**, p. 3703-3713, 1998.
8. M. S. Tsai and T. Y. Tseng, “Conduction mechanism and temperature-dependent current-voltage in $(Ba,Sr)TiO_3$ thin films”, *J. Electrochem. Soc.*, vol. **145**, pp. 2853, 1998.
9. C. S. Hwang, et. al., “Depletion layer thickness and Schottky type carrier injection at the interface between Pt electrodes and $(Ba, Sr)TiO_3$ thin films”, *J. Appl. Phys.*, vol **85**, pp. 287-295, 1999.
10. M. E. Lines and A. M. Glass, “Principles and applications of ferroelectrics and related materials”, pp. 534, Clarendon Press, Oxford, 1977.

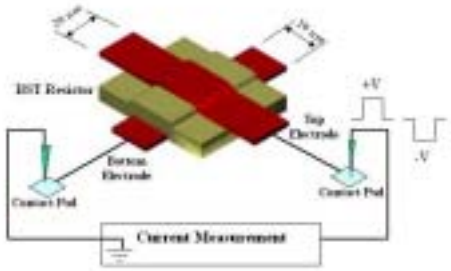

Fig. 1 Thin-film resistor of Pt/BST/Pt/TiN/Ti structure with intercrossing top/bottom electrodes for TCR testing

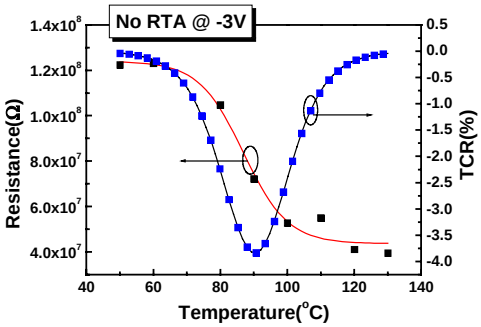

Fig. 2(a) TCR characteristic for the BST thin films without RTA at –3V.

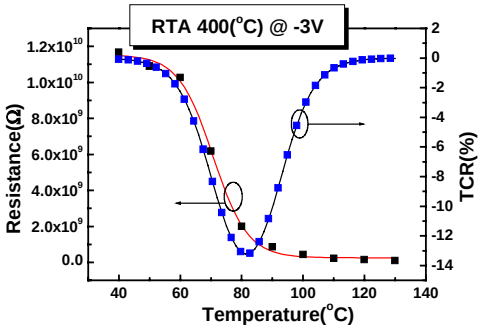

Fig. 2(b) TCR characteristic for the BST thin films with RTA 400°C at –3V.

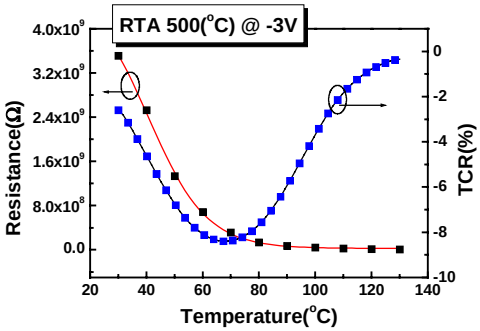

Fig. 2(c) TCR characteristic for the BST thin films with RTA 500°C at –3V.

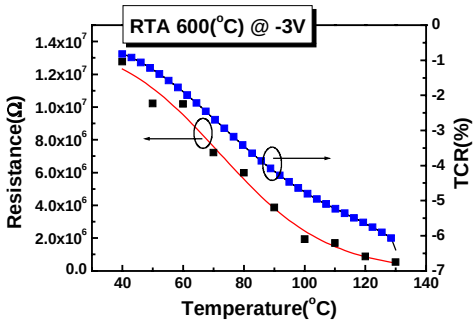

Fig. 2(d) TCR characteristic for the BST thin films with RTA 600°C at –3V.

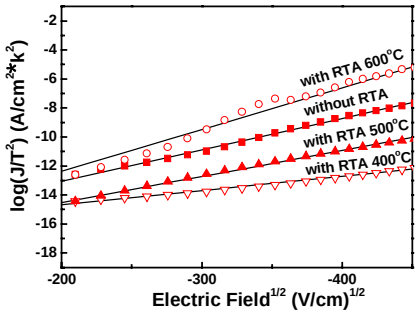

Fig. 3 log (J/T^2) vs. $E^{1/2}$ plots for the BST thin films treated with various RTA conditions at negative bias.

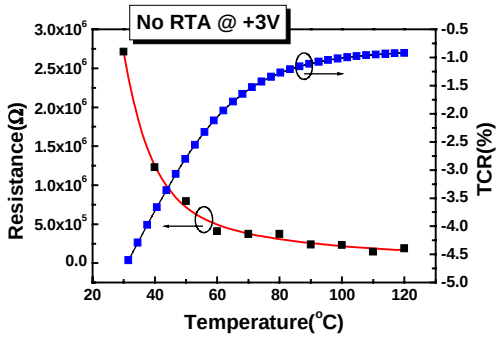

Fig. 4(a) TCR characteristic for the BST thin films without RTA at +3V.

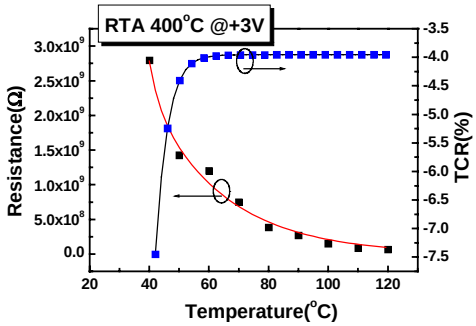

Fig. 4(b) TCR characteristic for the BST thin

films with RTA 400°C at +3V.

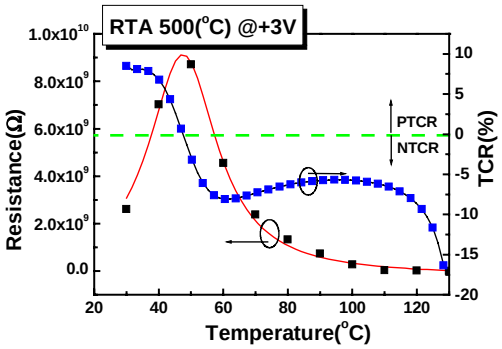

Fig. 4(c) TCR characteristic for the BST thin films with RTA 500°C at +3V.

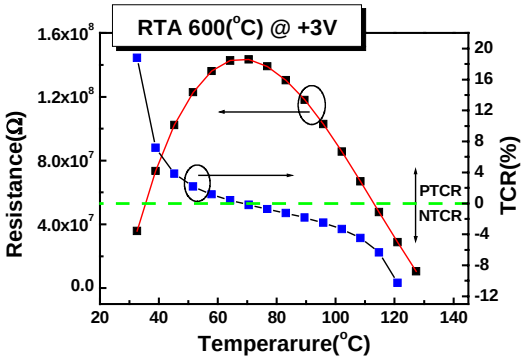

Fig. 4(d) TCR characteristic for the BST thin films with RTA 600°C at +3V.

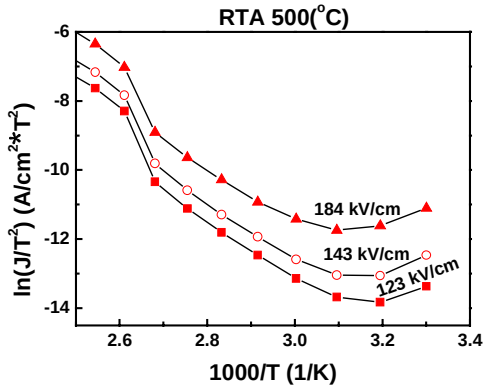

Fig. 5 log (J/T^2) vs. 1/T plots for the BST thin films with RTA 500°C at positive bias.

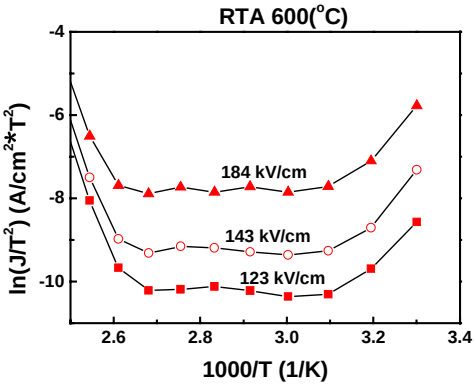

Fig. 6 log (J/T^2) vs. 1/T plots for the BST thin films with RTA 600°C at positive bias.

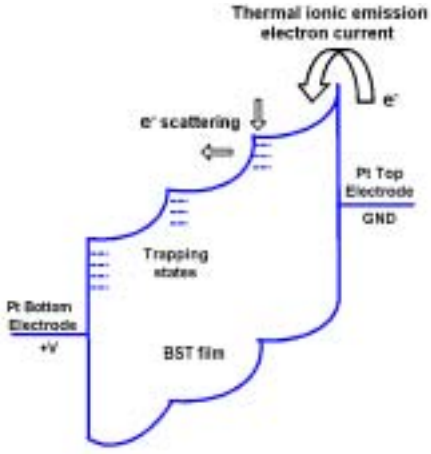

Fig. 7 Electron energy bands for RTA-treated BST films at negative bias.

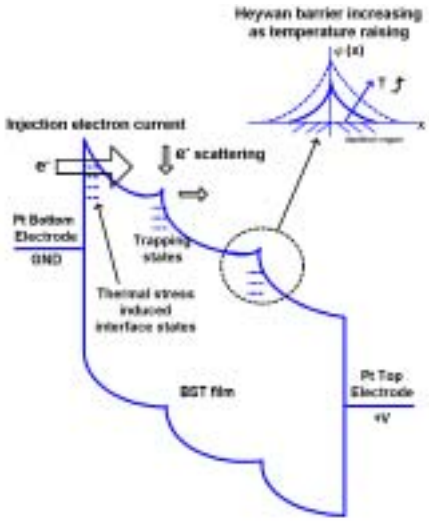

Fig. 8 Electron energy bands for RTA-treated BST films at positive bias.